The Human Erythrocyte Sugar Transporter Is Also a Nucleotide Binding Protein†

Anthony Carruthers* and Amy L. Helgerson
Department of Biochemistry, University of Massachusetts Medical School, 55 Lake Avenue North, Worcester, Massachusetts 01655

Received April 14, 1989; Revised Manuscript Received June 26, 1989

ABSTRACT: We have previously shown that ATP interacts with an intracellular, stereoselective, regulatory site(s) on the human erythrocyte sugar transport system to modify transport function in a hydrolysis-independent manner. This present study examines the nucleotide binding properties of the human erythrocyte sugar transport system. We demonstrate by transport studies in ghosts, by nucleotide binding studies with purified transport protein by measurements of nucleotide inhibition of 8-azidoadenosine 5′-[γ-^{32}P]triphosphate (azido-ATP) photoincorporation into purified carrier, and by analysis of nucleotide inhibition of carboxyl-terminal peptide antisera binding to purified glucose carrier than the glucose transport protein binds (with increasing order of affinity) AMP, ADP, ATP, 5′-adenylyl imidodiphosphate (AMP-PNP), and 1,N^6-ethenoadenosine 5′-triphosphate (EATP) at a single site. The carrier lacks detectable ATPase activity and GTP binding capacity. While AMP and ADP bind to the carrier protein and act as competitive inhibitors of ATP binding, these nucleotides are unable to mimic the ability of ATP, AMP-PNP, and EATP to modify the catalytic properties of the sugar transport system. Limited tryptic digestion of azido-ATP-photolabeled carrier suggests that the region of the glucose transport protein containing the intracellular cytochalasin B binding and extracellular bis(mannose) binding domains [residues 270–456; Holman, G. D., & Rees, W. D. (1987) *Biochim. Biophys. Acta 897*, 395–405] may also contain the intracellular ATP binding site.

Previous studies from this laboratory have shown that ATP interacts with the human erythrocyte glucose transport protein to reduce $K_{d(app)}$ for sugar binding to the external sugar binding site on the carrier protein and to increase $K_{d(app)}$ for sugar binding to the inward-facing sugar binding site (Carruthers, 1986a,b). In resealed red cell ghosts, intracellular ATP acts to reduce $K_{m(app)}$ and V_{max} for sugar uptake and to increase $K_{m(app)}$ for exit, leaving V_{max} for exit unchanged (Carruthers, 1986b; Hebert & Carruthers, 1986). ATP produces half-maximal effects upon ligand binding and sugar transport at approximately 50 μM ATP. The nonmetabolizable ATP analogue 5′-adenylyl imidodiphosphate (AMP-PNP)[1] can mimic ATP action on sugar transport in ghosts (Helgerson et al., 1989), but AMP, ADP, UTP, ITP, GTP, adenosine 5′-(α,β-methylenetriphosphate), and adenosine 5′-(β,γ-methylenetriphosphate) are unable to mimic ATP action (Carruthers, 1986a; Hebert & Carruthers, 1986). We concluded that ATP binds to a stereoselective, regulatory site on the glucose carrier to modify carrier function in a hydrolysis-independent fashion (Carruthers, 1986a).

In this study, we examine the ATP binding properties of the human erythrocyte glucose transport protein. We show that the carrier binds ATP with an apparent stoichiometry of 1 high-affinity ATP binding site per carrier, that the glucose transport protein contains no detectable ATPase activity, and that the carrier can be photolabeled using azido-ATP in an ATP-, ADP-, and AMP-inhibitable manner. Limited proteolysis of the photolabeled glucose carrier suggests that the region of the glucose carrier proposed to contain the intracellular cytochalasin B and extracellular sugar binding sites [residues 270–456 (Holman & Rees, 1987; Cairns et al., 1987)] also contains the region(s) of photoincorporation of azido-ATP. AMP and ADP appear to bind to the nucleotide binding site, increasing $K_{d(app)}$ for ATP binding to and modulation of the carrier, but alone are unable to mimic ATP action on transport.

Materials and Methods

Materials. 8-Azido[γ-^{32}P]ATP was purchased from ICN. [^{3}H]Cytochalasin B, [α-^{32}P]ATP, [γ-^{32}P]ATP, and [^{14}C]-3OMG were purchased from NEN. 1,N^6-Ethenoadenosine 5′-triphosphate was obtained from Molecular Probes, Inc. Rabbit antisera raised against a synthetic carboxyl-terminal peptide of the rat brain glucose transport protein (residues 480–492) were obtained from East Acres Biologicals. All remaining materials were purchased from Sigma unless stated otherwise.

Solutions. Tris medium consisted of 50 mM Tris-HCl, 2 mM $MgCl_2$, and 0.2 mM EGTA, pH 7.4. Saline consisted of 100 mM NaCl, 20 mM KCl, 10 mM $MgCl_2$, and 2 mM EGTA, pH 7.4. KCl medium consisted of 150 mM KCl, 2 mM $MgCl_2$, 2 mM EGTA, and 5 mM Tris-HCl, pH 7.4. Stopping solution was KCl medium (ice temperature) plus 1.5 mM KI, 1 μM $HgCl_2$, and 10 μM cytochalasin B. Lysis medium contained 10 mM Tris-HCl and 2 mM EGTA, pH 7.4.

Red Cell Ghosts. Red cell ghosts were prepared from washed, intact red cells as in Helgerson et al. (1989) using the KCl and lysis media described above. Red cell ghosts were depleted of peripheral membrane proteins by a single alkali wash as in Carruthers (1986b).

Sugar Transport Assays in Red Cell Ghosts. Unidirectional, zero-trans 3-*O*-methyl-α-D-[U-^{14}C]glucose uptake at

†This work was supported by National Institutes of Health Grant 2R01 DK36081.

* Author to whom correspondence should be addressed.

[1] Abbreviations: AMP-PNP, 5′-adenylyl imidodiphosphate; AMP-CPP, adenosine 5′-(α,β-methylenetriphosphate); AMP-PCP, adenosine 5′-(β,γ-methylenetriphosphate); azido-ATP, 8-azidoadenosine 5′-[γ-^{32}P]triphosphate, CCB, cytochalasin B; DFP, diisopropyl phosphorofluoridate; EATP, 1,N^6-ethenoadenosine 5′-triphosphate; EGTA, ethylene glycol bis(β-aminoethyl ether)-*N*,*N*,*N*′,*N*′-tetraacetic acid; 3OMG, 3-*O*-methyl-α-D-glucopyranoside; RBC, red blood cell; SDS-PAGE, sodium dodecyl sulfate–polyacrylamide gel electrophoresis; Tris-HCl, tris(hydroxymethyl)aminomethane hydrochloride.

0006-2960/89/0428-8337$01.50/0

ice temperature by red cell ghosts resealed and suspended in KCl medium was assayed as described previously (Helgerson et al., 1989).

Glucose Transport Protein. Glucose transport protein was purified from human erythrocytes as described in Cairns et al. (1984). The carrier is copurified with red cell lipid, and unsealed proteoliposomes are obtained upon removal of detergent (Carruthers, 1986a).

ELISA. ELISA was performed as by Sogin and Hinkle (1980) using 200 ng of purified glucose transport protein per well and serial dilutions (in the range 500–75 000-fold) of rabbit antisera (*C*-GT) raised against a synthetic carboxyl-terminal peptide of the rat brain glucose transport protein. Detergent (Tween-20) was omitted from all solutions to avoid potential denaturation of carrier and was replaced by inclusion of 1% bovine serum albumin (BSA) to reduce nonspecific adsorption of IgGs to the microtiter plates. Following adsorption of carrier (200 ng in 200 μL of 60 mM $NaCO_3$, pH 9.6, solution, 1–16 h at 37 °C) to the plates, each well was washed 3 times with phosphate buffer (20 mM sodium phosphate/145 mM NaCl, pH 7.5) and then additionally incubated with 200 μL of 1% BSA in carbonate buffer for 1 h at 37 °C. The reporter molecule for rabbit IgG binding to carrier was goat anti-rabbit IgG–peroxidase conjugate (Sigma, at 10 000-fold dilution). Bio-Rad peroxidase substrate kits were employed. Substrate development was arrested after 40 min using 1% oxalic acid and product determined by absorbance at 410 nm using a Dynatech MR 700 plate reader. Nonspecific IgG binding was determined by processing wells lacking glucose transport protein. IgG binding to carrier was performed ±ATP. In all other steps, ATP was absent.

Immunoprecipitations. Azido-ATP-photolabeled (see below) purified glucose carrier, red cell ghosts, or alkali-extracted red cell ghosts (Carruthers, 1986b) (100 μg of membrane protein) were solubilized overnight at 4 °C in Tris medium (500 μL) containing 2% NP-40 and 7 μL of *C*-GT. The suspension was then centrifuged for 1 h at 100000*g*, and the clear supernatant, which contained (in the case of purified glucose carrier) more than 90% of the original radioactivity, was retained. The supernatant fraction was then treated for 2 h at 4 °C with 25 μL of protein A–Sepharose beads (40 μg of protein A) preequilibrated with Tris medium plus 2% NP-40. The beads were sedimented by light centrifugation, and the supernatant was removed and counted. The pellet was washed 3 times in 1 mL of Tris medium plus NP-40, resuspended in 100 μL of distilled water, and counted.

Cytochalasin B Binding Assays. The procedure was that described by Helgerson and Carruthers (1987) for CCB binding to red cells and red cell ghosts with one modification. Purified carrier in [^{3}H]CCB medium was sedimented at 100000*g* for 10 min using a Beckman air centrifuge.

ATP Binding Studies. Purified carrier (100 μg, 1.82 nmol) in 55 μL of Tris medium was mixed with 55 μL of Tris medium containing variable [ATP] (0–2 mM, pH 7.4) plus [γ-^{32}P]ATP (20 μCi, 3 Ci/μmol, 60 nM). The suspension was placed on ice for 0–60 min. Carrier was sedimented by centrifugation for 10 min at 200000*g*, 3 × 5 μL aliquots of the supernatant were counted (as free ATP), and the remaining supernatant was aspirated. The pellet was resuspended in Tris medium containing 0.5% Triton X-100 and counted. Parallel experiments were performed using 2 μCi of [^{14}C]3OMG in place of [γ-^{32}P]ATP in order to estimate the water content of the pellet. Bound ATP was calculated as total [γ-^{32}P]ATP pellet space less [^{14}C]3OMG pellet space. Parallel cytochalasin B binding studies (see above) were made at 0 and 2 mM ATP. Time course studies indicate (1) ATP binding reached equilibrium within 5-min incubation on ice, and (2) [α-^{32}P]ATP binding to the carrier was quantitatively indistinguishable from [γ-^{32}P]ATP binding to the carrier.

Some experiments were performed in which we measured the binding of a fluorescent ATP derivative (EATP) to the glucose carrier. Here, carrier (60 μg in 25 μL of Tris medium added to 100 μL of Tris medium containing 5–50 μM EATP) was incubated at room temperature for 1 h and then centrifuged at 100000*g* for an additional hour. Samples of the clear supernatant were assayed for EATP content by fluorometry which was compared with an equivalent solution lacking glucose carrier. Control studies indicated that ATP and EATP binding to the centrifuge tubes was undetectable.

ATPase Assays. ATP hydrolysis at 24 °C was monitored by using the enzyme-linked procedure described in Schwartz et al. (1971). The reaction is

$$\mathrm{ATP} \xrightarrow{\text{ATPase}} \mathrm{ADP} + \mathrm{P_i}$$

$$\mathrm{PEP} + \mathrm{ADP} \xrightarrow{\text{pyruvate kinase}} \text{pyruvate} + \mathrm{ATP}$$

$$\text{pyruvate} + \mathrm{NADH} \xrightarrow{\text{lactate dehydrogenase}} \text{lactate} + \mathrm{NAD^+}$$

Glucose transport protein (500 μg) was resuspended in 1.5 mL of saline or Tris medium containing 500 μM ATP, 0.5 mM NADH, 2.5 mM phosphoenolpyruvic acid, 14 units of pyruvate kinase, and 20 units of lactate dehydrogenase (final carrier concentration 1.82 μM). Oxidation of NADH was monitored at 340 nm using a Hewlett Packard spectrophotometer. As positive controls, purified glucose transport protein was replaced with 100 μg of Na, K-ATPase (dog kidney, approximately 1 unit of activity/mg of protein, Sigma Chemicals). ATP assays were made by using the phosphoglycerate phosphokinase and glyceraldehydephosphate dehydrogenase coupled reaction assay (Sigma Chemicals).

Glucose Carrier Labeling by 8-Azido[γ-^{32}P]ATP. 8-Azido[γ-^{32}P]ATP is shipped in methanol. Methanol was blown off under N_2. Glucose transport protein or red cell ghosts (10–1000 μg of protein) were sedimented and resuspended to 250 μL in Tris medium containing variable [ATP] (0–2 mM). The protein suspension was then added to methanol-free 8-azido[γ-^{32}P]ATP (20–50 μCi, 16.6 Ci/mmol, 5–15 μM final concentration), gently vortexed, and equilibrated ±nucleotides on ice for 30 min. The suspension was then placed on an ice-cold plastic boat and irradiated from above for 0–120 s on ice using a UVG-11 Mineralight lamp (UVP Inc., 254 nm, 6 mW·cm^{-2} at a distance of 5–8 cm).

Proteolysis of Photolabeled Carrier. Glucose carrier (50 μg) photolabeled using 8-azido[γ-^{32}P]ATP was exposed to trypsin (1–4 μg) in Tris medium in the presence and absence of the protease inhibitor diisopropyl phosphorofluoridate (DFP, 1 mM) for 0–180 min. Unlabeled carrier (±1 mM Mg·ATP) was similarly treated. An equal volume of gel electrophoresis sample buffer (see below) containing 1 mM DFP was added to the protein suspension at an appropriate time and the mixture immersed in a boiling water bath for 90 s. The resulting peptides were separated by polyacrylamide gel electrophoresis (PAGE). These gels were then either processed for autoradiography (see below) or cut into slices for counting by liquid scintillation spectrophotometry or for further proteolysis of peptides. In the latter instance, gel lanes were sliced into appropriate lengths (generally 1–1.5-cm slices). Each slice was soaked in 45 mL of distilled water for 30 min and then placed in 1 mL of 50 mM NH_4HCO_3, pH 7.8. V8 protease (2 μg) was added, and the reaction vessels were placed on an orbital shaker at 20 °C for 4 h. A subsequent addition of V8

protease was made at this time and the reaction allowed to proceed overnight. The buffer was then collected, lyophilized, resuspended in sample buffer, and run on 20% acrylamide gels. The gel was then fixed (see below), silver stained, and processed for autoradiography. Control experiments demonstrated that ATP (2 mM) was without effect on the fragmentation of unlabeled carrier by trypsin.

Polyacrylamide Gel Electrophoresis (PAGE). Proteins were resolved either on 10% gels as described by Laemmli (1970) or, where separation of proteolytic fragments was required, on 20% acrylamide gels as described by Giulian et al. (1983). In the latter instance, gels were fixed by using glutaraldehyde (Giulian et al., 1983) to prevent loss of peptides below 10 kDa. For autoradiography, gels were scanned with a Hoefer Scientific gel scanner, dried, and then exposed to Kodak XAR-5 film at −70 °C for 2–48 h using a DuPont Cronex Lightning Plus intensifying screen.

Quantitation of Azido-ATP Incorporation into Carrier Resolved by PAGE. Purified glucose transport protein migrates as monomeric, dimeric, and multimeric species upon SDS–PAGE (see Figure 4). This assumed behavior was confirmed by using two methods. Electroelution of the monomeric species from gels followed by a second round of SDS–PAGE of the eluate results in the generation of monomeric, dimeric, and multimeric species. Lowering the pH of the sample buffer of the first round of SDS–PAGE to 4.0 markedly reduces the quantity of dimer and multimer detected and increases the monomeric content of protein without loss of total protein. Quantitations reported here are with respect to the azido-ATP content of monomeric carrier resolved upon SDS–PAGE.

Loading gel lanes with identical quantities of carrier was problematic—this may result from adsorption of proteoliposomes to plastic- and glassware. Following SDS–PAGE, each gel was stained and destained and the amount of monomeric carrier per lane quantitated by integration of densitometry scans. Over the range of protein concentrations used in this study (5–50 μg), protein staining is a linear function of [protein] although uncertainties in absolute [protein] exist (see above). The gels were then dried and subjected to autoradiography and the autoradiographs analyzed by densitometry. The monomeric component of each lane (autoradiograph) was then corrected for the small variations in protein content detected in scans of the stained gel. In other experiments following scanning of the stained gel, each lane was excised, cut into 2-mm slices which were then dissolved, and counted for ^{32}P content by liquid scintillation spectrometry.

Terminology. In this study, we refer to K_d, $K_{d(app)}$, K_i, and $K_{i(app)}$ for nucleotide interaction with glucose carrier and the glucose transport system. For clarity, the following distinctions (but deviations from accepted nomenclature) apply. $K_{d(app)}$ and $K_{i(app)}$ refer to parameters measured in the presence of competitive inhibitors. K_d and K_i refer to $K_{d(app)}$ and $K_{i(app)}$, respectively, following correction for competitive inhibition. For example, $K_i = K_{i(app)}/(1 + [S]/K_S)$ where [S] and K_S refer to the concentration of and the K_d for an interfering species. We have no evidence that K_d and K_i parameters reported here reflect true K_d and K_i parameters for the interactions we describe.

Results

Which Nucleotides Modify Sugar Transport Activity in Red Cell Ghosts? Previous studies from this laboratory have suggested a strict nucleotide specificity for sugar transport modulation by nucleotides—ATP and AMP-PNP alone appear to modulate sugar transport (Carruthers, 1986a; Helgerson et al., 1989). Table I summarizes the effects of a variety of intracellular nucleotides on 0.1 mM 3OMG uptake by red blood cell ghosts. As the net effect of saturating intracellular ATP on 3OMG uptake at ice temperature is to reduce $K_{m(app)}$ and V_{max} for 3OMG uptake in ATP-free ghosts by some 8-fold (Helgerson et al., 1989), the expected effect of ATP_i on sugar uptake from media containing subsaturating sugar is transport stimulation.

Table I: Effects of Nucleotides on 0.1 mM 3-*O*-Methylglucose Uptake by Human Red Cell Ghosts[a]

condition	3OMG uptake[b] (μmol L^{-1} min^{-1})	SD	n[c]	P[d]
red blood cells	12.2	1.6	8	NSD
ATP-"free" ghosts[e]	2.8	0.3	16	$p < 0.005$
ATP-"free" ghosts + 1 mM ATP_o[f]	2.9	0.4	4	$p < 0.005$
ghosts + 1 mM AMP_i	1.8	0.3	8	$p < 0.005$
ghosts + 1 mM ADP_i[g]	13.9	1.9	4	NSD
ghosts + 1 mM ATP_i	13.7	2.1	16	
ghosts + 1 mM $EATP_i$	16.5	2.6	4	NSD
ghosts + 1 mM AMP-PNP_i	12.7	1.9	4	NSD
ghosts + 1 mM GTP_i	3.4	0.2	4	$p < 0.005$
ghosts + 1 mM AMP-CPP_i	2.7	0.1	4	$p < 0.005$

[a] 3-*O*-Methylglucose uptake was measured at ice temperature (0–4 °C). Uptake was measured in intact cells or in ghosts lacking or containing exogenous nucleotides which were added during the resealing step. All solutions contained $MgCl_2$ (2 mM) and EGTA (2 mM). [b] Uptake is defined as that component of total uptake which was inhibited by 10 μM cytochalasin B (>95% in all cases shown here). [c] The number of determinations made in duplicate. [d] One-tailed *t* test of the hypothesis that uptake is significantly less than that observed in ATP-containing ghosts. The results either indicate that there is no significant difference (NSD) or indicate the level of significance of the observed reduction in uptake. [e] Ghosts resealed in the absence of exogenous ATP (intracellular [ATP] ≈2 – 20 μM). [f] Subscripts o and i refer to extra- and intracellular locations, respectively. [g] ADP (1 mM)-resealed ghosts contain detectable ATP levels (460 μM) by the time of transport assay.

Resealing ghosts in the presence of ADP, ATP, EATP, or AMP-PNP (each at 1 mM) result in significant stimulation of sugar uptake. AMP_i, GTP_i, and AMP-CPP_i (each at 1 mM) fail to mimic the action of ATP_i on 3OMG uptake by ghosts. Previous studies with inside-out red cell membrane vesicles (Carruthers, 1986a; Hebert & Carruthers, 1986) have demonstrated that extravesicular AMP, ADP, UTP, GTP, ITP, AMP-CPP, and AMP-PCP (at 1 mM) are without effect on sugar exit from vesicles while ATP (1 mM) is a marked inhibitor of sugar exit. The anomalous finding in this study is the ability of ADP_i to mimic the action of ATP_i on sugar uptake by red cell ghosts. This effect of ADP in ghosts could be explained by red cell membrane vesiculation-induced alterations in transport function. A more likely explanation is that in the absence of AMP_i, residual adenylate kinase activity associated with ghosts (Tsuboi, 1978) converts ADP_i to ATP_i. Consistent with this hypothesis is the observation that ADP-loaded ghosts contain significant levels of ATP following resealing [Table I; see also Jacquez (1983)].

Table I shows that uptake by ghosts containing exogenous AMP but lacking exogenous ATP is significantly lower than uptake by ghosts lacking exogenous nucleotides. This raises the possibility that either AMP_i inhibits sugar transport at low [3OMG] or AMP, while unable to mimic ATP action on transport, competes with residual endogenous ATP_i for interaction with the transport system. Figure 1 summarizes experiments in which we evaluated the effects of AMP_i on ATP_i (150 μM) stimulation of 0.1 mM 3OMG uptake by red cell ghosts at ice temperature. In the absence of exogenous ATP_i, AMP_i reduces 3OMG uptake in a saturable manner

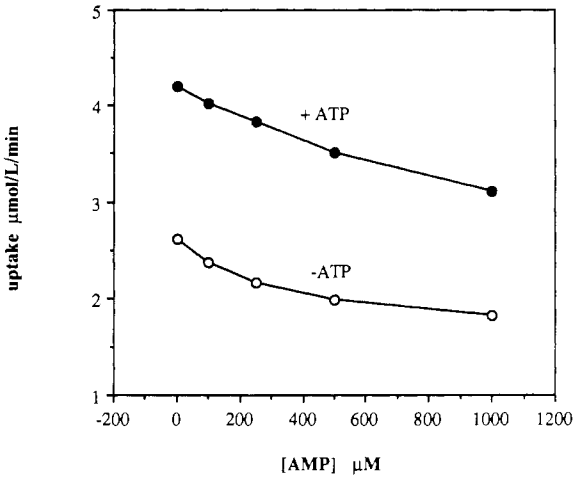

FIGURE 1: Partial reversal of ATP action on red cell ghost 3OMG uptake by intracellular AMP. Ordinate: 3OMG uptake (at 0.1 mM 3OMG) in micromoles per liter of cell water per minute. Abscissa: [AMP] present during resealing ghosts. Ghosts were resealed in the absence (open circles) or presence (filled circles) of 150 μM ATP. AMP was also present during the resealing step at the concentrations indicated. Uptake of 3OMG (0.1 mM) was measured at ice temperature. The curves are drawn by eye. Each point represents the mean of two determinations made in duplicate.

with $K_{i(app)}$ = 221 μM. Resealing ghosts in the presence of 150 μM ATP_i increases 3OMG uptake, an effect partly reversed by including AMP in the resealing medium. In the presence of 150 μM ATP_i, AMP_i reduces uptake with $K_{i(app)}$ of 503 μM. These data suggest that AMP_i can compete with ATP_i for interaction with the transport system but is unable to mimic the action of ATP on transport. In the simplest possible scenario where AMP and ATP compete for binding to a single site (K_d for ATP binding = 45 μM; see below) but where AMP lacks transport-modulating capacity, the K_i for AMP inhibition of ATP (150 μM) interaction with the transport system would be 116 μM.

Does the Glucose Carrier Bind ATP? The above experiments demonstrate that intracellular nucleotides modify the catalytic activity of the human red cell glucose transport system. While previous results from this laboratory suggest that ATP binds to purified glucose carrier with a $K_{d(app)}$ of 40–45 μM (Carruthers, 1986a), this conclusion is based upon the use of a single methodological approach and remains to be confirmed by independent procedures.

Figure 2 summarizes four separate experiments in which we measured the [ATP] dependence of ATP binding to the purified glucose transport protein (100 μg in 110 μL) using either [γ-^{32}P]ATP or [α-^{32}P]ATP as reporter molecules for binding. The results obtained using either reporter molecule were indistinguishable. The data in Figure 2 are presented in Scatchard form and are consistent with two components of ATP binding. The "high affinity" component of binding is characterized by $K_{d(app)}$ of 42 ± 8 μM and $[E]_{total}$ = 1.41 ± 0.16 nmol of binding sites. The second component of binding is nonsaturable, running parallel to the abscissa of the Scatchard plot, indicating nonspecific adsorption of labeled ATP to the proteoliposomes. Nonspecific binding is characterized as [bound ATP] = k[ATP] where k = 0.55 μmol (nmol of glucose transport protein)$^{-1}$ (mol of ATP)$^{-1}$. In parallel experiments, we determined that cytochalasin B binding to the purified glucose transport protein (100 μg in 110 μL of Tris medium) was characterized by K_d of 144 nM and $[E]_{total}$ = 1.47 ± 0.06 nmol of binding sites. ATP (1 mM) was without significant effect on the cytochalasin B binding capacity of the purified carrier. The ratio of saturable ATP binding sites

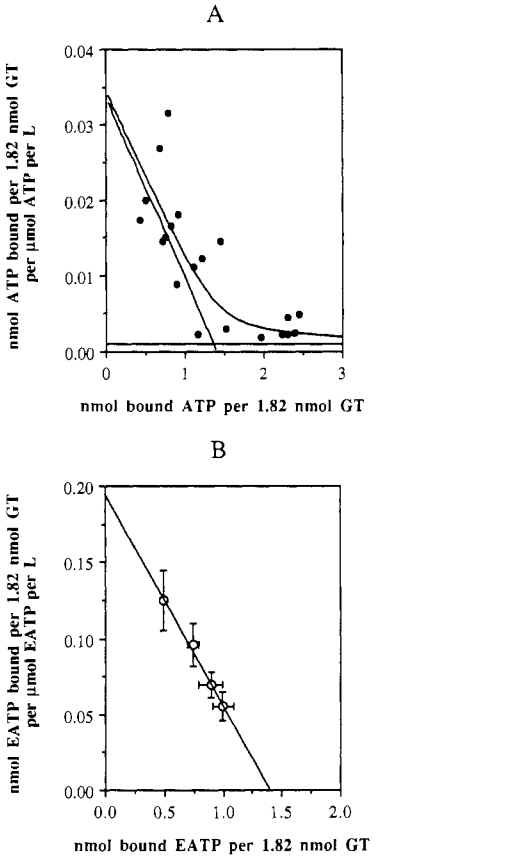

FIGURE 2: Scatchard analysis of nucleotide binding to the purified glucose transport protein. (A) ATP binding to the carrier. Ordinate: nanomoles of ATP bound per 1.82 nmol of glucose carrier per micromole of free ATP per liter. Abscissa: nanomoles of ATP bound per 1.82 nmol of glucose carrier. Each point represents a separate measurement made in duplicate. The data (in the form [bound ATP] versus [free ATP]) were analyzed by the nonlinear method of Marquardt (1963) to obtain components of ATP binding. Two models were tested: (1) a saturable component of binding plus a nonspecific component of binding ([bound ATP] = $\{B_{max}[ATP]/(K_d + [ATP])\}$ + k[ATP]); (2) two components of saturable binding ([bound ATP] = $\{B_{max1}[ATP]/(K_{d1} + [ATP])\} + \{B_{max2}[ATP]/(K_{d2} + [ATP])\}$). The first model provided a final solution with a lower χ^2 value, suggesting a significantly better fit. The curves drawn through the data points are based upon acceptance of the first model. The curve running parallel to the abscissa represents nonspecific ATP binding [k = 0.55 μmol of ATP (nmol of glucose carrier)$^{-1}$ (mol of ATP)$^{-1}$]. The remaining linear curve represents saturable binding with K_d = 42 μM ATP and B_{max} = 1.41 nmol of ATP binding sites per 1.82 nmol of glucose carrier. The nonlinear curve represents total binding (saturable plus nonspecific). Acceptance of the first model is supported experimentally by our inability to inhibit residual [γ-^{32}P]ATP binding by very high levels (>4 mM) of unlabeled ATP. (B) EATP binding to the glucose carrier. Ordinate and abscissa as in (A). The curve drawn through the points represents the least-squares fit to the data which is consistent with a single, saturable component of EATP binding with K_d = 7 μM and B_{max} = 1.46 nmol of EATP binding sites per 1.82 nmol of glucose carrier. The data points represent mean ± 1 SD of quadruplicate estimates.

to cytochalasin B binding sites is 0.96 ± 0.15. The ratios of saturable ATP binding sites and cytochalasin B binding sites per mole of carrier protein are 0.77 ± 0.09 and 0.81 ± 0.03, respectively, assuming an average molecular weight for the glucose transport protein of 55K.

The red cell nucleotide transporter is known to copurify with glucose carrier (Jarvis & Young, 1981), but only 4% of total protein is accounted for by nucleoside carrier. Thus, unless the nucleoside carrier contains 20–25 high-affinity ATP binding sites per carrier, the observed ATP binding must be quantitatively accounted for by binding to the glucose carrier.

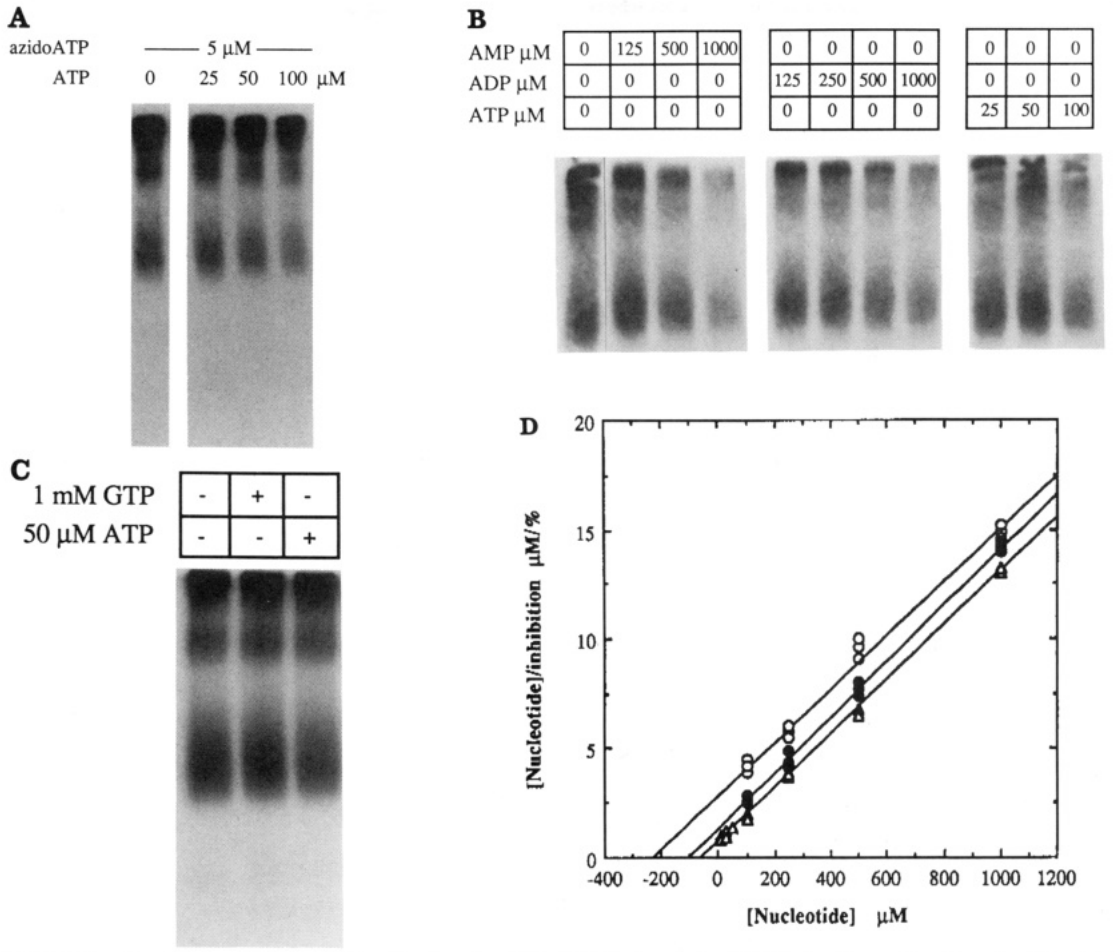

FIGURE 3: Photolabeling the glucose carrier with 8-azidoadenosine 5′-[γ-^{32}P]triphosphate. (A) Autoradiographs of carrier (25 μg) photolabeled with 5 μM azido-ATP. Carrier, preequilibrated with azido-ATP and unlabeled ATP (0, 25, 50, and 100 μM) for 30 min on ice, was UV irradiated for 1 min and then resolved by SDS–PAGE and the dried gel subjected to autoradiography. (B) As in (A). Here, however, the carrier (50 μg) was preequilibrated with 15 μM azido-ATP ± various concentrations of AMP, ADP, or ATP. The concentrations of these nucleotides are shown above the appropriate gel lane. Two gels were run simultaneously; lanes 1 and 9–11 were from gel 2 and lanes 2–8 from gel 1. (C) Failure of GTP to inhibit azido-ATP incorporation into glucose carrier. Carrier was exposed to azido-ATP (15 μM), to label plus GTP (1 mM), or to label plus ATP (50 μM), irradiated for 1 min, resolved by SDS–PAGE, and then subjected to autoradiography. (D) Quantitation of inhibition of azido-ATP photoincorporation into glucose carrier by AMP, ADP, and ATP. Ordinate: [nucleotide]/inhibition (μM/%) Abscissa: [nucleotide] (μM). Data are shown for AMP (open circles), ADP (filled circles), and ATP (open triangles) inhibition of photoincorporation. The lines drawn through the points were calculated by least squares and extrapolate to $-K_{i(app)}$ on the abscissa. Each point was obtained from a separate experiment. The slope of each line is indistinguishable, corresponding to maximum inhibition of photoincorporation by nucleotide of approximately 80%.

Under the equilibrium binding conditions employed in this study, we were unable to detect significant ^{32}P associated with the carrier subsequently resolved upon SDS–PAGE.

Figure 2 also summarizes experiments in which EATP (a fluorescent ATP derivative) binding to the glucose carrier was determined. EATP binds to the carrier with a K_d of 7 μM and a B_{max} of 0.8 mol/mol of carrier. Insufficient data points are available for analysis of low-affinity or nonspecific EATP binding to glucose carrier in these experiments. Assuming a nonspecific, carrier EATP binding capacity identical with that of ATP, nonspecific EATP binding would account for only 2% of total binding at the highest [$EATP_{free}$] employed (18 μM).

Partial Characterization of the Glucose Carrier ATP Binding Site. (A) Affinity Labeling of the Carrier with a Photoreactive ATP Analogue. UV irradiation of purified glucose carrier preequilibrated with 8-azido[γ-^{32}P]ATP (15 μM) results in photoincorporation of ^{32}P into carrier protein. In the absence of irradiation, no measurable ^{32}P is incorporated into the carrier protein. At the shortest irradiation period tested (≈1–2 s), photolabel incorporation is quantitatively indistinguishable from incorporation following 120-s irradiation. Figure 3 shows that AMP, ADP, and ATP but not GTP inhibit azido-ATP incorporation into carrier. Inhibition of photolabeling by ATP is half-maximal at 59 ± 7 μM ATP. AMP and ADP inhibit azido-ATP labeling of glucose transport protein half-maximally at 212 ± 29 and 105 ± 16 μM, respectively. Assuming the K_d for azido-ATP binding to the carrier is identical with the K_d for ATP binding (45 μM) and simple competition between AMP, ADP, ATP, and azido-ATP for binding to the carrier, K_i values for AMP, ADP, and ATP inhibition of azido-ATP photoincorporation are 159 ± 22, 79 ± 12, and 44 ± 5 μM, respectively. Only 0.3–0.6% of total carrier is labeled by 8-azido[γ-^{32}P]ATP in the absence of ATP. Assuming again that the K_d for azido-ATP binding to the carrier is identical with that of ATP binding (an assumption supported by the previous calculations), only 25% of the carrier binds the photolabel (at 15 μM) prior to irradiation. This provides an upper estimate of 1–2% efficiency of incorporation of photolabel.

Control experiments show that at least 75% of the radioactivity associated with detergent (NP-40)-solubilized, azido-ATP-photolabeled band 4.5 protein (100 μg) is immunoprecipitated by antisera raised against the C-terminal 13

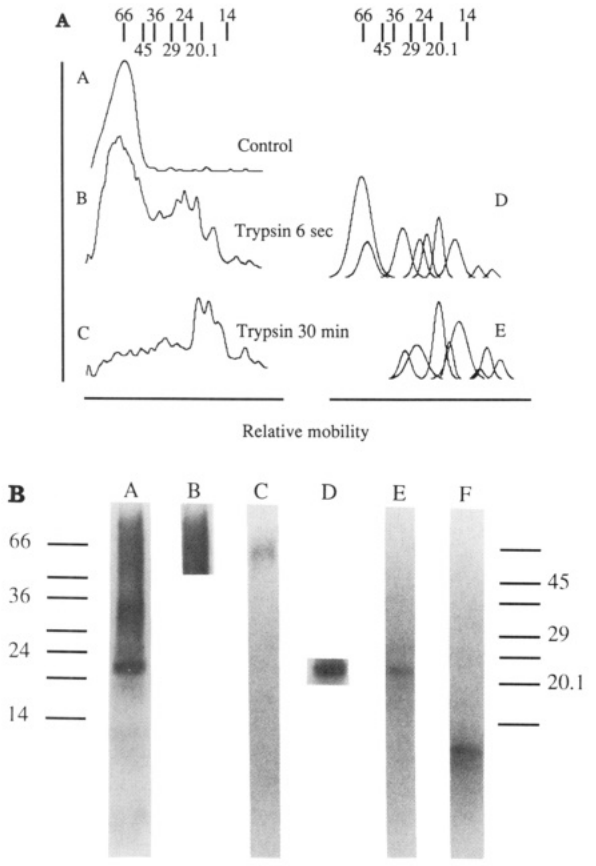

FIGURE 4: Proteolysis of azido-ATP-labeled carrier. (A) Labeled carrier (50 μg) was exposed to trypsin (1 μg) for 6 s (B, D) or 30 min (C, E). Proteolysis was arrested by addition of 1 mM DFP in sample buffer followed by boiling. Control (A) and proteolyzed carrier were resolved by SDS–PAGE (20% acrylamide), and the gel was subjected to autoradiography. The resulting autoradiographs were analyzed by scanning densitometry (A–C) and resulting peaks identified by Gaussian integration (D, E). (B) Proteolysis of the labeled, 21-kDa tryptic fragment by V8 protease. The gel slice containing the 21-kDa tryptic peptide (lane A) was excised from the gel (lane D) and exposed to 0 (lane E) or 2 μg (lane F) of V8 protease in NH_4HCO_3 (pH 7.8) at 20 °C for 4 h. A subsequent addition of V8 protease was made to lane F peptide, and both reactions (E and F) were allowed to proceed overnight. The buffer was collected, lyophilized, and run on a 20% SDS–polyacrylamide gel. Following fixation and silver staining, the gel was subjected to autoradiography. That region of lane A containing nonproteolyzed carrier was excised (lane B), treated as in lane E, and then resolved on a subsequent 20% gel (lane C). The positions of molecular weight markers are indicated to the left and right of the autoradiographs.

residues (480–492) of rat brain glucose carrier. As maximal competitive inhibition of photolabel incorporation into carrier protein by ATP, ADP, and AMP is approximately 80%, this suggests that label is incorporated predominantly into glucose carrier and not into the contaminating nucleoside carrier.

(B) Proteolysis of 8-Azido[γ-^{32}P]ATP-Labeled Carrier. In this section, we evaluate whether limited proteolysis of azido-ATP-labeled glucose carrier results in the release of specific, labeled peptides.

The human erythrocyte glucose carrier is rapidly hydrolyzed by trypsin. Within 6 s of exposure to trypsin (1:30 trypsin: carrier ratio by weight) at room temperature, the photolabeled carrier is cleaved to produce labeled peptides of M_r 34K, 28K, 25K, 21K, 16.6K, 11.9K, and 9.7K (Figure 4). Further exposure (30 min) to trypsin results in the loss of the 25-kDa peptide and the generation of additional peptides of M_r 17.8K and 10.3K. Endo F treatment of carrier reduces the apparent molecular weight of labeled carrier from 55K to 48K but is without effect on the mobility of labeled tryptic peptides, suggesting that these peptides are not extensively glycosylated. Trypsin treatment of azido-ATP-labeled purified carrier results in a small loss (13%) of label associated with the proteoliposomes. The remaining activity is associated with the sedimentable lipid/protein pellet.

The peptide of M_r 21K is a major peptide containing photolabel. V8 protease treatment of the gel slice containing this peptide produces a faintly labeled peptide of appM_r 11.8 K (Figure 4). The remaining label (which was confirmed to elute from the gel upon V8 protease treatment) could not be resolved upon PAGE.

ATP Modifies Anti-Rat Brain Glucose Carrier Carboxyl-Terminal Antisera Binding to Human Red Cell Glucose Carrier. Antisera raised against the C-terminal 13 residues (480–492) of rat brain glucose carrier bind to an intracellular moiety of the human erythrocyte glucose transport protein (Haspel et al., 1988). Here we ask does ATP binding to the glucose carrier affect the ability of these antisera (*C*-GT) to bind to the carboxyl terminus of the human erythrocyte glucose transport protein.

Mg·ATP interferes with the ability of *C*-GT to bind to purified glucose transport protein adsorbed to ELISA plates (Figure 5). Figure 5A shows the time course of *C*-GT (20 nL of *C*-GT serum per 200 μL of phosphate buffer) binding to 200 ng of glucose carrier ±1 mM Mg·ATP. While ELISA is unlikely to provide the most sensitive assay of the time course of IgG binding to carrier, the data show that *C*-GT binding at short incubation intervals is significantly depressed by the presence of ATP. As the duration of exposure of carrier to *C*-GT is increased, binding is less affected by the presence of ATP. At 60 min, *C*-GT binding to carrier ±ATP are indistinguishable. The approach we adopted in the experiments described below was to measure the effects of nucleotides on *C*-GT binding to carrier at times where differences between binding ±ATP are detectable (e.g., at 30 min). The ATP concentration dependence of ATP reduction of *C*-GT binding to the carrier was determined in four separate experiments at two dilutions of *C*-GT (10 000- and 50 000-fold). These experiments are summarized in Figure 5B. ATP half-maximally reduces *C*-GT binding to carrier at 45.7 ± 4.5 μM. AMP, ADP, UTP, ITP, and AMP-CPP alone (at 1000 μM) are much less effective than ATP in their ability to reduce *C*-GT binding to carrier (Figure 5B).

Control experiments using polyclonal rabbit antisera (δ-GT) raised against purified glucose transport protein demonstrate that δ-GT binding and *C*-GT binding are additive and that ATP is without significant effect on δ-GT binding to glucose carrier. This suggests that δ-GT and *C*-GT bind to dissimilar, independent sites on the glucose carrier and that only binding of *C*-GT is sensitive to the presence of ATP. AMP-PNP and EATP (5–50 μM) are more potent inhibitors than ATP of *C*-GT binding to carrier (Figure 5B) with $K_{i(estimated)}$ values of 22.3 ± 4.3 and 12.7 ± 0.9 μM, respectively. These latter parameters were estimated by nonlinear regression (Duggleby, 1981) but are less reliable as insufficient data points were obtained at high nucleotide concentrations.

AMP and ADP (250–1000 μM) reduce the effects of ATP (500 μM) on *C*-GT binding to the glucose carrier (Figure 5C). Assuming simple competition between ATP and AMP and between ATP and ADP for binding to the carrier with complete reversal of ATP inhibition by AMP and ADP, we calculate K_i values for AMP and ADP inhibition of ATP action on *C*-GT binding of 122 ± 21 and 79 ± 8 μM, respectively.

Does the Glucose Carrier Contain ATPase Activity? Purified glucose transport protein (500 μg in 1.5 mL of saline

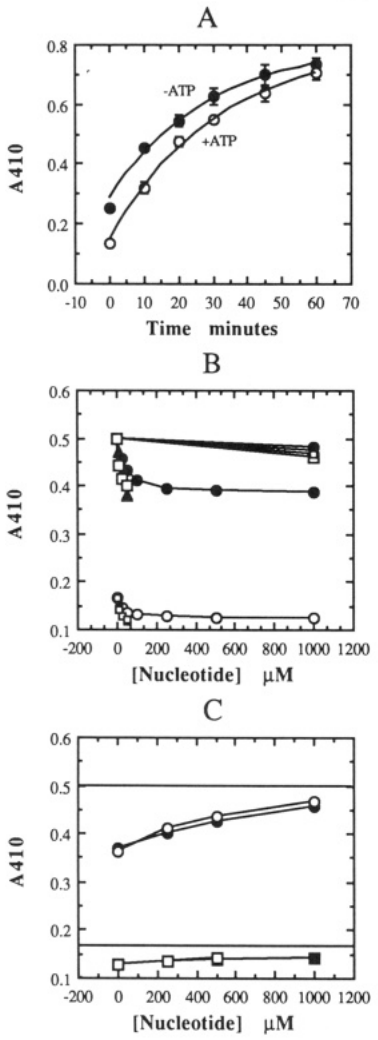

FIGURE 5: Effects of nucleotides on *C*-GT binding to purified glucose carrier. (A) Time course of *C*-GT binding ±1 mM Mg·ATP. Ordinate: absorbance at 410 nm. Abscissa: time in minutes. Data are shown for binding in the absence (filled circles) and presence (open circles) of ATP. Data points are shown as mean ± 1 SD of four separate experiments. The curves drawn through the points were obtained by a least-squares analysis of the data assuming binding is a monoexponential process. Control, absorbance = $0.52(1 - e^{-0.035t}) + 0.287$; +ATP, absorbance = $0.65(1 - e^{-0.031t}) + 0.147$. (B) Effects of nucleotides on *C*-GT binding to carrier. Ordinate as in (A). Abscissa: nucleotide concentration, μM. *C*-GT binding was allowed to proceed for 35 min. Each data point represents the mean of six or more separate determinations. Data are shown for two dilutions of *C*-GT (10000- and 50000-fold). The upper cluster of data points ($A_{410} > 0.3$) represents the results of measurements at 10000-fold dilution of *C*-GT and the lower points ($A < 0.3$) those obtained at a 50000-fold dilution of *C*-GT. Considering the upper points first, those nucleotides resulting in significant inhibition in A_{410} at concentrations below 200 μM are ATP (filled circles), EATP (open squares), and AMP-PNP (filled triangles). Those nucleotides whose effects were measured only at 1000 μM nucleotide are AMP, ADP, UTP, ITP, and AMP-CPP. The results shown for a 50000-fold dilution of *C*-GT represent inhibition by ATP (open circles), EATP (open squares), and AMP-PNP (filled squares). (C) Reversal of ATP inhibition of *C*-GT binding by AMP and ADP. Ordinate and abscissa as in (C). In this experiment, *C*-GT binding was measured at 10000-fold (open and filled circles) and 50000-fold (open and filled squares) dilutions of *C*-GT. *C*-GT was allowed to bind to carrier for 35 min. All binding was performed in the presence of ATP (500 μM), but [AMP] (filled symbols) or [ADP] (open symbols) concentrations were progressively increased. Each data point is the mean of six or more separate determinations. The straight lines running parallel to the abscissa represent the level of *C*-GT binding to the carrier in the absence of ATP (*C*-GT at 10000-fold dilution, upper line and *C*-GT at 50000-fold dilution, lower line).

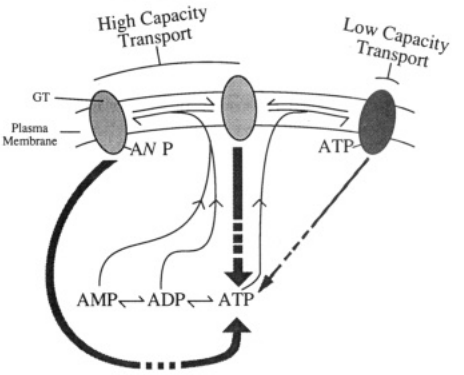

FIGURE 6: Working model for nucleotide control of red cell sugar transport. Plasma membrane glucose carrier (GT) can exist in an unliganded form or liganded to ATP or to AMP or ADP. The nucleotide-free form of the carrier (GT) and the AMP- or ADP-liganded carrier (GT-A*N*P) result in high-capacity sugar transport by red cells. The ATP-liganded carrier confers low-capacity sugar transport to the red cell. Synthesis of ATP by the red cell from glucose (shown by the discontinuous arrows) favors GT-ATP formation and low-capacity sugar transport. ATP hydrolysis results in ADP and AMP formation which compete with ATP for binding to the carrier and drive the equilibrium toward GT-A*N*P high-capacity sugar transport.

or Tris medium; 60 μM carrier) shows no detectable ATPase activity. Positive controls employing dog kidney (Na, K)-ATPase (100 μg, Sigma Chemicals) demonstrate significant ATPase activity (1.6 μmol of ATP mg^{-1} min^{-1}) inhibited by ouabain (50 μM) and by Na and K removal from the incubation medium.

Discussion

The results of this study support the hypothesis that ATP modulation of the catalytic and ligand binding properties of the human erythrocyte glucose transport protein may be mediated via interaction with a stereospecific, nucleotide binding site on the glucose transport protein (Carruthers, 1986a,b; Hebert & Carruthers, 1986). This site displays low affinity (K_i for inhibition of azido-ATP photoincorporation >1 mM) for GTP but binds AMP, ADP, ATP, AMP-PNP, and EATP with K_i values of 132, 79, 45, 20, and 10 μM, respectively. Once bound to the glucose transport protein, ATP seems not to be hydrolyzed to ADP. Studies with glucose carrier C-terminal peptide antisera suggest that ATP binding induces subtle changes in carrier structure or that bound ATP interferes directly in IgG binding.

While AMP and ADP compete with azido-ATP for binding to the sugar transport protein nucleotide binding site, these nucleotides are unable to mimic ATP, AMP-PNP, and EATP in their ability to modify sugar transport (Carruthers, 1986a). This raises the possibility that AMP and ADP can compete with ATP for binding to the carrier and thereby diminish the effects of intracellular ATP on erythrocyte sugar transport. This hypothesis is supported by the demonstration that AMP competitively inhibits the action of ATP on erythrocyte sugar transport. It is possible, therefore, that ATP hydrolysis can result in transport stimulation by two routes: (1) ATP dissociation from the carrier, and (2) AMP and ADP competition with ATP for binding to the carrier. This model is summarized in Figure 6. In the absence of AMP and ADP, V_{max} for sugar uptake would be half-maximal at ≈45 μM ATP_i. At physiologic $[AMP]_i$ and $[ADP]_i$ (19 and 220 μM, respectively; Ericson et al., 1983), $K_{i(app)}$ for ATP inhibition of transport, $K_{d(ATP)}(1 + [AMP]/K_{d(AMP)} + [ADP]/K_{d(ADP)})$, would be 180 μM ATP, a value close to that observed for ATP modulation

of sugar transport in squid giant axons (Baker & Carruthers, 1981).

An unresolved question at this time is whether ATP is the sole cytosolic species necessary for full expression of sugar transport modulation by ATP. A recent study by Wheeler (1989) concludes that ATP is without effect on sugar transport in liposomes containing reconstituted, human erythrocyte, whole membrane proteins. Our studies demonstrate that ATP modifies sugar transport in human red cell ghosts and inside-out membrane vesicles (Carruthers, 1986a,b; Hebert & Carruthers, 1986; Helgerson et al., 1989; see Table I here). In addition, this current study and previous studies from this laboratory demonstrate that ATP interacts with high affinity with the glucose carrier (Carruthers, 1986a,b). A number of explanations could account for the divergent findings reported by Wheeler (1989) and here. (1) ATP modulation of sugar transport may involve additional, unidentified species which are dysfunctional or absent in the reconstitution studies reported by Wheeler (1989). (2) It is possible that the form of reconstituted carrier studied by Wheeler (1989) in the absence of Ca^{2+}-chelating agents is the Ca^{2+}-inhibited form shown to be insensitive to allosteric regulation by nucleotides (Helgerson et al., 1989). (3) Glucose carrier reconstituted by the procedure of Wheeler (1989) may be dysfunctional with respect to transport and/or ATP modulation of transport.

The latter possibility seems likely. The turnover number for reconstituted glucose transporter in the studies of Wheeler (1989) is only some 5–10% of the activity observed in red cell membranes. This unexpected difference in native and reconstituted carrier activities cannot be accounted for by arguments based upon reconstitution efficiency. Even if only 10% of glucose transport proteins are functionally reconstituted by this procedure, those vesicles containing functional carrier should equilibrate with extravesicular sugar at a rate consistent with the activity observed in native membranes.

We have suggested (Carruthers, 1986a) that ATP inhibition of transport in extensively washed red cell inside-out membrane vesicles is less than that produced by cytosol-containing ATP. In addition, our reconstitution studies have demonstrated a requirement for cytosolic protein in ATP inhibition of transport.[2] Cytosolic protein alone was without effect on reconstituted transport.[2] ATP could, therefore, promote interactions of glucose carrier with additional cellular elements. This possibility remains to be fully evaluated.

Examination of the deduced primary structure of the HepG2 glucose transport protein—a protein shown to share extensive homology with the human erythrocyte glucose carrier protein (Mueckler et al., 1985)—indicates the presence of three potential consensus ATP binding sequences (Table II). Consensus sequence I is shared by several ATPases and GTPases as well as by DNA A protein, Epstein–Barr virus protein, thymidine kinase, cAMP-dependent protein kinase, phospholipase A2, glycogen phosphorylase, and nitrogenase (Fry et al., 1986). Consensus sequence II bears weak homology to corresponding portions of these proteins and strong homology to adenylate kinase and to regions of the protein kinases and transcarboxylase (Fry et al., 1986). Consensus sequence III has counterparts in the sequences of adenylate kinase and the ATP/ADP translocase (Fry et al., 1986). Studies with adenylate kinase (Fry et al., 1986) suggest that consensus sequence II forms part of the pocket in which the adenine ribose moiety of Mg·ATP is located and that consensus sequence III flanks the triphosphate chain of Mg·ATP. How these sequences relate to glucose transporter interaction with ATP (if at all) remains to be established. Indeed, the suggested secondary structure of the HepG2 glucose carrier locates consensus sequence I within a transmembrane domain (Mueckler et al., 1985). We calculated the probability of random occurrence of each consensus sequence within the HepG2 protein knowing the amino acid composition of the protein. These are listed in Table II. The probability of all three consensus sequences occurring randomly is 2.6×10^{-11} and in the correct order (I–II–III) is 4.4×10^{-12}. It should be noted, however, that similar probabilities could be obtained for other, conserved regions of the glucose carrier.

The HepG2 ATP binding consensus sequence III is a highly conserved domain shared by a family of suggested transport proteins (Table II). Consensus sequences I and II are, however, less conserved in human fetal muscle (Kayano et al., 1988), human (Thorens et al., 1988) and rat (Fukumoto et al., 1988) liver, and rat adipose insulin-regulated (James et al., 1989) glucose transport proteins. The high-affinity, glucose-repressable SNF3 glucose transport protein of yeast (Celenza et al., 1988) shows only weak homology with HepG2 carrier consensus sequences I–III.

Limited tryptic digestion of proteoliposomes containing azido-ATP-photolabeled carrier results in the generation of a number of peptides containing label. Tryptic peptides

Table II: Consensus Sequences of ATP Binding Proteins[a]

Sequence[b]	Protein[c]	Residues	p[d]
G X X X X G K	**Consensus Sequence I**		
| | |			
G F S K L **G** **K**	HepG2/rat brain	111-117	2.6×10^{-4}
G C S K F **G** P	Rat Liver	141-147	
G L C K V A **K**	Human Fetal Skeletal Muscle	109-115	
G L A N A A A	Rat Adipocyte Insulin Regulated	127-133	
Q V G A G **G** I	Yeast SNF3	189-195	
K X V X K	**Consensus Sequence II**		
| | |			
K S **V** L **K**	HepG2/rat brain	225-229	8×10^{-5}
K K S L **K**	Rat Liver	255-259	
K Q **I** L Q[e]	Human Fetal Skeletal Muscle	223-227	
R K S L **K**	Rat Adipocyte Insulin Regulated	241-245	
K S - L S	Yeast SNF3	302-305	
G X X X L X L	**Consensus Sequence III**		
| | |			
G R R T **L** H **L**	HepG2/rat brain	332-338	1.3×10^{-3}
G R R T **L** F **L**	Rat Liver	362-368	
G R R T **L** F M	Human Fetal Skeletal Muscle	330-336	
G R R T **L** H **L**	Rat Adipocyte Insulin Regulated	348-354	
G R R K V L V	Yeast SNF3	416-422	

[a] Consensus ATP binding sequences were obtained from Fry et al. (1986). [b] Peptide amino acid sequence is shown in the one-letter amino code. Amino acids showing identity or homology with consensus sequences are shown in boldface. [c] The sugar transport proteins listed here are HepG2 and rat brain carriers (Mueckler et al., 1985; Birnbaum et al., 1986), rat and human liver carriers (Thorens et al., 1988; Fukomoto et al., 1988), human fetal skeletal muscle carrier (Kayano et al., 1988), adipose and heart carrier (James et al., 1989), and yeast SNF3 carrier (Celenza et al., 1988). [d] The probability of observing this sequence by chance was calculated by knowing the amino acid composition of the HepG2 glucose transport protein. [e] Consensus sequence II requires a hydrophobic third residue. This requirement is satisfied by isoleucine.

[2] A. L. Helgerson and A. Carruthers, unpublished observations.

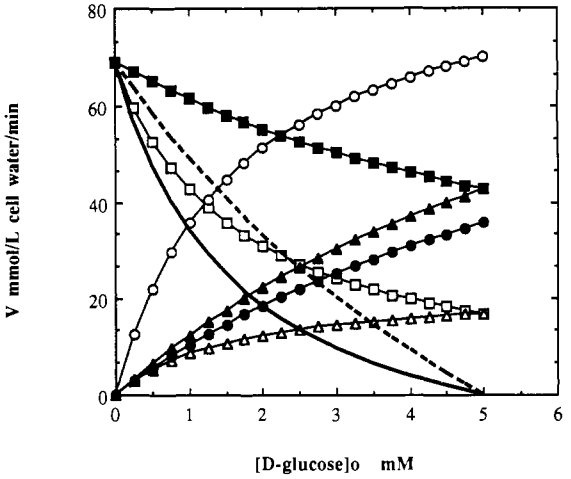

FIGURE 7: Transport components mediated by a fixed (two)-site carrier (Helgerson & Carruthers, 1989). Ordinate: rate of transport (millimoles per liter of cell water per minute). Abscissa: external [D-glucose] in millimolar. Internal [D-glucose] is 5 mM. Net glucose exit is given by net exit = $\{[V^{12}(S_1/K_1) + V^{ee}(S_1S_2/K_1K_2)] - [V^{21}(S_2/K_2) + V^{ee}(S_1S_2/K_1K_2)]\}/[1 + (S_1/K_1) + (S_2/K_2) + (S_1S_2/K_1K_2)]$ where V, K, and S refer to V_{max}, $K_{m(app)}$, and D-glucose concentrations, respectively, subscripts 1 and 2 refer to intra- and extracellular locations, and superscripts 12, 21, and ee refer to transport directions in to out, out to in, and exchange, respectively. For net fluxes, the exchange components are identical and may be dropped. The open symbols refer to transport components in red cells containing 1.6 mM ATP and the closed symbols to transport components in ATP-free cells. The squares indicate unidirectional exit rates mediated by carrier occupied by sugar at the internal site only, the triangles indicate unidirectional uptake rates by carrier occupied by sugar at the external site only, and the circles indicate unidirectional exchange rates (carrier occupied by intra- and extracellular sugar). Total unidirectional uptake and exit are given by the sum of uptake and exchange rates and by the sum of exit and exchange rates, respectively. Net exit (exit − uptake) in the presence and absence of ATP_i is shown by the continuous and discontinuous curves (no symbols), respectively. The transport parameters used (+ATP) were those measured at 20 °C for V^{12}, V^{21}, V^{ee}, K_1, and K_2 of 180, 36, and 240 mmol L^{-1} min^{-1} and 8 and 1.6 mM, respectively (Naftalin & Holman, 1977). In the absence of ATP, we assumed K_2 and V^{21} parameters of 8 mM and 180 mmol L^{-1} min^{-1}, respectively (i.e., transport is symmetric).

corresponding to residues 213–269 and 457–492 are released from the proteoliposomes and may be isolated by centrifugation of the digest and collection of the supernatant (Cairns et al., 1987). The pellet retaining all remaining peptides contains 87% of the original photolabel, indicating that peptides 213–269 and 457–492 are not major sites of photoincorporation of azido-ATP. A major peptide produced upon tryptic digestion of the glucose carrier runs with an apparent molecular weight of 21K. This peptide has been identified as residues 270–456 (Cairns et al., 1987) of M_r 20.5K. This region of protein contains the inward-facing cytochalasin B binding site (Deziel & Rothstein, 1984) tentatively assigned close to Trp-412 (Deziel et al., 1984), the external ASA–BMPA (sugar) binding site tentatively assigned to residues 359–368 (Holman & Rees, 1987), and the inward-facing ATP binding consensus sequence III (residues 332–338). V8 protease cleavage of the 21-kDa-labeled peptide under conditions favoring cleavage at Glu-X (Drapeau, 1977) results in the generation of a labeled peptide of appM_r 11.8K. This peptide could correspond to residues 270–380 (11.9 kDa) which contain ATP binding consensus sequence III. Precise localization of the point(s) of photoincorporation of azido-ATP into the human erythrocyte sugar transport protein will require purification and sequencing of labeled peptides.

The significance of ATP modulation of human red cell glucose transport to red cell physiology is unclear. The human red cell has 15 000-fold greater transport than glucose metabolic capacity, and intracellular glucose content is normally in equilibrium with extracellular glucose (Jacquez, 1984). Our studies have shown that ATP confers transport asymmetry to red cells, the principle effect being to decrease $K_{m(app)}$ and V_{max} for sugar uptake (Carruthers & Melchior, 1983; Carruthers, 1986b). In the nominal absence of ATP_i, transport in red cells appears to be symmetric [$V_{max(exit)} = V_{max(entry)}$; Carruthers & Melchior, 1983; Carruthers, 1986b]. This has an interesting consequence with respect to net sugar fluxes from red cells. Consider a hypothetical situation in which red cells containing 5 mM D-glucose are suddenly exposed to serum containing 0–5 mM D-glucose. In Figure 7 we calculate the various components of transport (sugar uptake, exit, and exchange transport) that can occur via a fixed-site transporter (Helgerson & Carruthers, 1989). While net sugar exit falls with increasing external sugar (transport is passive), net exit from ATP-free cells (cells where transport is symmetric) is greater than from cells containing physiologic (1.6 mM) ATP levels (cells where transport is asymmetric). This arises because less carrier is involved in futile exchange. Although these calculations are hypothetical and assume arbitrary constraints with respect to sugar and ATP_i levels, these considerations suggest that under conditions of metabolic impoverishment, red cells could deliver more glucose to tissues.

Of more general significance is the demonstration that many tissues contain human erythrocyte-type glucose transport protein in addition to specialized carrier isoforms involved in regulatory pathways (e.g., insulin-translocated carrier in adipose; James et al., 1988, 1989; Thorens et al., 1988). Should the red cell type carrier found in these tissues also possess nucleotide binding capacity of the type described in this present study, this would provide the potential for sugar transport regulation by ATP-dependent control of the activity of red cell type sugar transport proteins already in situ at the cell membrane. This type of regulation would be distinct from regulation by translocation of intracellular carrier proteins to the plasma membrane (James et al., 1988).

Registry No. AMP, 61-19-8; ADP, 58-64-0; ATP, 56-65-5; AMP-PNP, 25612-73-1; EATP, 37482-17-0.

REFERENCES

Baker, P. F., & Carruthers, A. (1981) *J. Physiol. (London) 316*, 503–525.

Bangham, A. D., Standish, M. M., & Watkins, J. C. (1965) *J. Mol. Biol. 13*, 238–245.

Birnbaum, M. J., Haspel, H. C., & Rosen, O. M. (1986) *Proc. Natl. Acad. Sci. U.S.A. 83*, 5784–5788.

Cairns, M. T., Elliot, D. A., Scudder, P. R., & Baldwin, S. A. (1984) *Biochem. J. 221*, 179–188.

Cairns, M. T., Alvarez, J., Panico, M., Gibbs, A. F., Morris, H. R., Chapman, D., & Baldwin, S. A. (1987) *Biochim. Biophys. Acta 905*, 295–310.

Carruthers, A. (1986a) *J. Biol. Chem. 261*, 11028–11037.

Carruthers, A. (1986b) *Biochemistry 25*, 3592–3602.

Carruthers, A., & Melchior, D. L. (1983) *Biochim. Biophys. Acta 728*, 254–266.

Celenza, J. L., Marshall-Carlson, L., & Carlson, M. (1988) *Proc. Natl. Acad. Sci. U.S.A. 85*, 2130–2134.

Deziel, M. R., & Rothstein, A. (1984) *Biochim. Biophys. Acta 776*, 1020.

Deziel, M., Pegg, W., Mack, E., Rothstein, A., & Klip, A. (1984) *Biochim. Biophys. Acta 772*, 403–406.

Drapeau, G. R. (1977) *Methods Enzymol. 47*, 189–191.

Duggleby, R. G. (1981) *Anal. Biochem. 110*, 9–18.

Ericson, A., Niklasson, F., & de Verdier, C. (1983) *Clin. Chim. Acta 127*, 47-59.
Fry, C., Kuby, S. A., & Mildvan, A. S. (1986) *Proc. Natl. Acad. Sci. U.S.A. 83*, 907-911.
Fukomoto, H., Seino, S., Imura, H., Seino, Y., Eddy, R. L., Fukushima, Y., Byers, M. G., Shows, T. B., & Bell, G. I. (1988) *Proc. Natl. Acad. Sci. U.S.A. 85*, 5434-5438.
Giulian, G. G., Moss, R. L., & Greasner, M. (1983) *Anal. Biochem. 129*, 277-287.
Haspel, H. C., Rosenfeld, M. G., & Rosen, O. M. (1988) *J. Biol. Chem. 263*, 398-403.
Hebert, D. N., & Carruthers, A. (1986) *J. Biol. Chem. 261*, 10093-10099.
Helgerson, A. L., & Carruthers, A. (1987) *J. Biol. Chem. 262*, 5464-5475.
Helgerson, A. L., & Carruthers, A. (1989) *Biochemistry 28*, 4580-4594.
Helgerson, A. L., Hebert, D. N., Naderi, S., & Carruthers, A. (1989) *Biochemistry 28*, 6410-6417.
Holman, G. D., & Rees, W. D. (1987) *Biochim. Biophys. Acta 897*, 395-405.
Jacquez, J. A. (1983) *Biochim. Biophys. Acta 727*, 367-378.
Jacquez, J. A. (1984) *Am. J. Physiol. 246*, R289-R298.
James, D. E., Brown, R., Navarro, J., & Pilch, P. F. (1988) *Nature 333*, 183-185.
James, D. E., Strube, M., & Mueckler, M. (1989) *Nature 338*, 83-87.
Jarvis, S. M., & Young, J. D. (1981) *Biochem. J. 194*, 331-338.
Jung, C. Y., Carlson, L. M., & Whaley, D. A. (1971) *Biochim. Biophys. Acta 241*, 613-627.
Kayano, T., Fukomoto, H., Eddy, R. L., Fan, Y., Byers, M. G., Shows, T. B., & Bell, G. I. (1988) *J. Biol. Chem. 263*, 15245-15248.
Laemmli, U. K. (1970) *Nature 270*, 680-685.
Marquardt, D. W. (1963) *SIAM J. Appl. Math. 11*, 431-441.
Mueckler, M., Caruso, C., Baldwin, S. A., Panico, M., Blench, I., Morris, H. R., Allard, W. J., Lienhard, G. E., & Lodish, H. F. (1985) *Science 229*, 941-945.
Naftalin, R. J., & Holman, G. D. (1977) in *Membrane transport in red cells* (Ellory, J. C., & Lew, V. L., Eds.) pp 257-300, Academic Press, New York.
Schwartz, A., Nagano, K., Nakao, M., Lindenmyer, G. E., Allen, J. C., & Matsui, H. (1971) *Methods Pharmacol. 1*, 368-371.
Sogin, D. C., & Hinkle, P. C. (1980) *Proc. Natl. Acad. Sci. U.S.A. 77*, 5725-5729.
Taverna, R. D., & Langdon, R. G. (1973) *Biochim. Biophys. Acta 298*, 422-428.
Thorens, B., Sarkar, H. K., Kaback, H. R., & Lodish, H. F. (1988) *Cell 55*, 281-290.
Tsuboi, K. K. (1978) *Methods Enzymol. 51*, 467-473.
Wheeler, T. J. (1989) *Biochemistry 28*, 3413-3420.

Cross-Linking of β-Bungarotoxin to Chick Brain Membranes. Identification of Subunits of a Putative Voltage-Gated K^+ Channel†

Ralf R. Schmidt and Heinrich Betz*
ZMBH, Universität Heidelberg, Im Neuenheimer Feld 282, D-6900 Heidelberg, FRG
Received April 10, 1989; Revised Manuscript Received June 20, 1989

ABSTRACT: β-Bungarotoxin (β-Butx), a presynaptically active neurotoxin from snake venom, is thought to bind to a subtype of voltage-gated K^+ channels. ^{125}I-β-Butx was cross-linked to its high-affinity binding site in membrane fractions from chick brain by using the bivalent reagents 1-ethyl-3-[3-(dimethylamino)propyl]carbodiimide and sulfosuccinimidyl 6-[(4-azido-2-nitrophenyl)amino]hexanoate. Two major adducts of apparent M_r 90 000–95 000 and 46 000–49 000 were obtained with both cross-linkers. Formation of both adducts was inhibited by the K^+ channel ligands dendrotoxin I and mast cell degranulating peptide. Our data indicate that the putative β-Butx-sensitive neuronal K^+ channel contains at least two different types of subunits of about 75 and 28 kDa.

K^+ channels regulate the membrane potential of many animal cells and represent a highly diverse family of transmembrane proteins. In excitable tissues, voltage-dependent K^+ channels control the duration of action potentials, cardiac pacemaking, and neurotransmitter secretion from presynaptic nerve endings (Hille, 1984). Through the use of mutants and specific neurotoxins, K^+ channel proteins have recently become amenable to molecular genetic and biochemical analysis [reviewed in Jan and Jan (1989) and Dolly (1988)]. In *Drosophila*, different A-type K^+ channel subunits have been shown to result from alternative splicing of the complex "*shaker*" gene locus (Pongs et al., 1988; Schwarz et al., 1988). In the same organism, a family of *shaker*-related genes has recently been identified which may encode other K^+ channel subtypes (Butler et al., 1989). For mammalian brain and muscle, evidence for the heterogeneity of K^+ channels mainly comes from electrophysiological and pharmacological data (Hille, 1984).

β-Bungarotoxin (β-Butx)[1] is a basic protein from snake venom composed of two disulfide-linked subunits of M_r 13 500 and 7000 (Kelly & Brown, 1974). The toxin exhibits Ca^{2+}-dependent phospholipase A_2 activity and potently inhibits

† This work was supported by the Deutsche Forschungsgemeinschaft (SFB 317) and the Fonds der Chemischen Industrie. R.R.S. was supported by the Landesgraduiertenförderungsprogramm of Baden-Württemberg.
* To whom correspondence should be addressed.

[1] Abbreviations: β-Butx, β-bungarotoxin; Dtx-I, dendrotoxin I; MCDP, mast cell degranulating peptide; EDAC, 1-ethyl-3-[3-(dimethylamino)propyl]carbodiimide; SSANPAH, sulfosuccinimidyl 6-[(4-azido-2-nitrophenyl)amino]hexanoate; EDTA, ethylenediaminetetraacetic acid; HEPES, *N*-(2-hydroxyethyl)piperazine-*N*'-2-ethanesulfonic acid; SDS-PAGE, sodium dodecyl sulfate-polyacrylamide gel electrophoresis.

0006-2960/89/0428-8346$01.50/0